

# Dynamic facilitation observed near the colloidal glass transition

Scott V. Franklin\*

*Department of Physics, Rochester Institute of Technology, Rochester, NY, 14623-5603, USA*

Eric R. Weeks†

*Department of Physics, Emory University, Atlanta, Georgia 30322, USA*

(Dated: April 4, 2024)

We present experimental confirmation of dynamic facilitation in monodisperse and bidisperse colloidal suspensions near the glass transition volume fraction. Correlations in particle dynamics are seen to exist not only in space (clusters and strings) but also as bubbles in space-time. Quantitatively, highly mobile particles are more likely (than immobile particles) to have nearest neighbors that were highly mobile in immediately preceding times. The interpretation is that a particle's mobility enables or facilitates the subsequent motion of its neighbors. Facilitation is most pronounced at the relaxation time that corresponds with cage-breaking, when dynamic heterogeneity is also maximized.

PACS numbers: 64.70.pv, 61.43.Fs, 66.10.cg

As the temperature in a supercooled liquid is lowered, the dynamics slow dramatically and, at a well-defined temperature, the system becomes a glass[1–3]. The glass is amorphous, with no long-range molecular ordering. In liquid samples close to the glass transition, molecular motion becomes slow and spatially heterogeneous [4–6], occurring through localized groups of molecules simultaneously rearranging [7, 8]. Approaching the glass transition, the frequency of these motions drops and the length scales characterizing the groups of rearranging particles increases [4, 8, 9].

Garrahan and Chandler[10, 11] proposed a model that posits the correlation of particle mobility not only in space but also in space-time. In the *dynamic facilitation* model, motion by a group of particles at one time facilitates *subsequent* motion of particles in adjacent regions. Dynamic facilitation clusters, “bubbles” in space-time [12], are distinct from conventional clusters or strings of moving particles [8], which are spatially correlated only over a single time interval. These space-time clusters can be quite large [13], showing that local groups of mobile particles are more than just a single-time random event.

Vogel and Glotzer [14] found evidence for dynamic facilitation in molecular dynamics simulations of viscous silica. They observed that mobile particles, rather than randomly distributed throughout the sample, were more likely to be found next to a previously mobile particle. They quantified this with a dynamic facilitation parameter  $F(\Delta t)$ , defined as the increased probability of a particle mobile over time  $\Delta t$  having a previously mobile nearest neighbor, as compared to the null hypothesis of the previously mobile particles being randomly distributed. In their simulations, decreasing the temperature brought about the development of a pronounced peak in  $F(\Delta t)$  at a delay time corresponding to the cage-rearrangement time scale. Quantitatively, mobile particles were 1.5 to 2 times more likely than non-mobile particles to have had at least one previously mobile nearest neighbor. There

has been, however, no direct experimental confirmation of dynamic facilitation.

Colloidal suspensions provide a promising model system to test the prediction of facilitated mobility. Colloids are composed of micron-sized solid particles in a liquid. Our interest is in colloidal glasses, similar to hard sphere glasses in that temperature plays no role in the glass transition, its effects limited to particle Brownian motion [15]. Instead, the control parameter for each sample is the particle volume fraction  $\phi$ . Colloids have a glass transition at  $\phi_g \approx 0.58$ , and are liquid-like at volume fractions below this threshold [15, 16]. The colloidal glass transition shares many similarities to the traditional glass transition [16], such as a dramatically growing viscosity [17], increasing relaxation time scales [18, 19], and amorphous structure similar to a liquid [20]. Most relevant for dynamic facilitation, colloidal samples can be viewed directly with confocal microscopy: experiments observed dynamic heterogeneity with long-range spatial correlations [21–23]. While these experiments found growing dynamical length scales as the glass transition was approached, the fundamental dynamics in question were all within a specific time interval, probing simultaneous spatial correlations of motion. Testing the dynamic facilitation model, however, requires the comparison of motion in two successive time intervals.

In this Letter we examine previously published data from confocal experiments on colloidal samples close to the colloidal glass transition [22, 23]. These data sets are 3D observations of the trajectories of several thousand particles per sample. We find dynamic facilitation occurs in these samples, with the Vogel-Glotzer parameter reaching values similar to that seen in simulations [14].

*Experimental methods* — We re-analyze data reported on previously in Refs. [22, 23], which should be consulted for complete experimental details. Both experiments involved colloidal poly-(methymethacrylate) particles sterically stabilized by a thin layer of poly-12-

hydroxystearic acid. Weeks *et al.* studied a nominally monodisperse sample particles with mean diameter  $d = 2.36 \mu\text{m}$  [22]; Narumi *et al.* a nominally bidisperse mixture of small ( $d = 2.36 \mu\text{m}$ ) and large ( $d = 3.01 \mu\text{m}$ ) particles with a number ratio of  $N_S/N_L = 1.56$  [23]. All particles for both experiments were produced at the University of Edinburgh by Andrew Schofield, and each particle species had a polydispersity of 5% [22, 23].

We focus on data from liquid-like samples with  $0.4 \leq \phi \leq \phi_g$ .  $\phi$  was determined from counting particles seen in three-dimensional (3D) confocal microscope images, as described below. Uncertainties in the mean particle diameters result in systematic uncertainties of the volume fraction [24] of  $\pm 0.03$  for the monodisperse samples and  $\pm 0.02$  for the bidisperse samples. As in the prior publications, we report volume fractions to two significant digits (e.g.,  $\phi = 0.55$ ), and they are accurate to this extent relative to each other for a given colloid type (monodisperse or bidisperse) [24]. These particles are slightly charged, but nonetheless the glass transition for each of these experimental data sets is  $\phi_g \approx 0.58$  [22, 23].

Colloidal particles were imaged using confocal microscopy. 3D image stacks were acquired on time scales sufficiently fast that particle motion was minimal between each stack, which was straightforward given the slow dynamics of the dense samples. Particle motion was tracked in 3D using standard techniques [25, 26]. For the monodisperse case, particle positions are determined to  $\pm 0.03 \mu\text{m}$  in  $x$  and  $y$ , and  $\pm 0.05 \mu\text{m}$  in  $z$  [22, 26]. For the bidisperse case, the uncertainties were higher,  $\pm 0.2 \mu\text{m}$  in  $x$  and  $y$ , and  $\pm 0.3 \mu\text{m}$  in  $z$  [23]. This was due to the difficulty of tracking both particle sizes simultaneously.

The mean square displacement (MSD) gives a sense of the relevant time scales and is shown in Figs. 1(a) and 2(a) for the monodisperse and bidisperse samples respectively. At time scales shorter than shown ( $\Delta t \lesssim 1 \text{ s}$ ), particle motion is diffusive. At intermediate time scales the MSD's show a plateau that develops with increasing volume fraction. This represents cage-trapping in which particle motion is constrained by nearest neighbors. At longer time scales, the cages rearrange and particles move to new locations [22, 23]. The rearrangement time scale also corresponds to the time scale in which displacement probability distributions are broader than a Gaussian. This is quantified by the non-Gaussian parameter  $\alpha_2$ , defined as  $\alpha_2(\Delta t) = (\langle \Delta x^4 \rangle / 3 \langle \Delta x^2 \rangle^2) - 1$  [7, 27]. This parameter is zero for a Gaussian distribution, and positive when the tails of the distribution are more probable than expected for a Gaussian.  $\alpha_2(\Delta t)$  is shown in Figs. 1(b) and 2(b). Note that we compute both the MSD and  $\alpha_2$  using only the  $x$  and  $y$  displacements as they have less particle tracking uncertainty than the  $z$  component. The non-Gaussian parameter  $\alpha_2(\Delta t)$  peaks at a time scale  $\Delta t^*$ , matching the end of the plateaus in the MSD's.

The larger particle displacements occurring on this time scale  $\Delta t^*$  involve spatially localized groups of par-

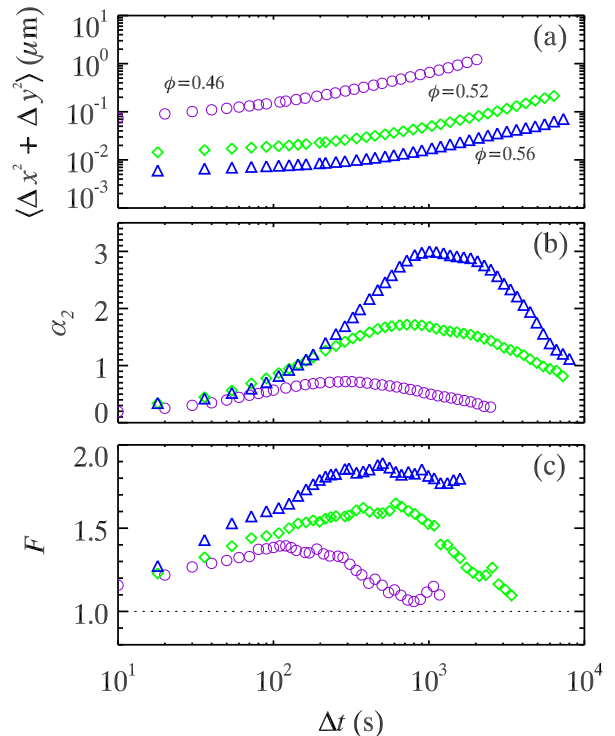


FIG. 1. (color online) (a) Mean-squared displacements (MSD) of three different volume fractions as indicated, of a monodisperse colloidal suspension. (b) Non-Gaussian parameter and (c) dynamic facilitation parameter for the samples. The symbols are the same in all three panels, defined as shown in (a).

ticles [7, 8, 21–23]. Particles at a given moment in time with unusually large displacements are typically observed in clusters, as shown in Fig. 3 and discussed in detail in Refs. [8, 21–23]. All particles, even those not rearranging on the time scale  $\Delta t^*$ , are continually undergoing Brownian motion, and the displacements of those that are truly rearranging are not much larger than that of the caged particles [22]. To best highlight the mobile particles we consider a modified form of the displacement vector first used by Donati *et al.* [8]:

$$\delta r(t_0, \Delta t) = \max_{t_1, t_2} |\vec{r}(t_1) - \vec{r}(t_2)| \quad (1)$$

with  $t_0 \leq t_1 < t_2 \leq t_0 + \Delta t$ . This maximal displacement removes effects due to random motions within a cage and better captures the net particle displacement. Using this definition for mobility  $\delta r$ , we show the 5% most mobile particles at two moments in time in Fig. 3. The blue particles are mobile in the first time interval, the red in the second, and purple in both. Clusters of mobile particles are seen in several locations. Red and blue particles appear in similar locations; nearest neighbors (defined below) are indicated by black bonds. These are the particles for which dynamic facilitation may play a role.

**Dynamic Facilitation** — Following Vogel and Glotzer, we define two time intervals of duration  $\Delta t$ : the “past”

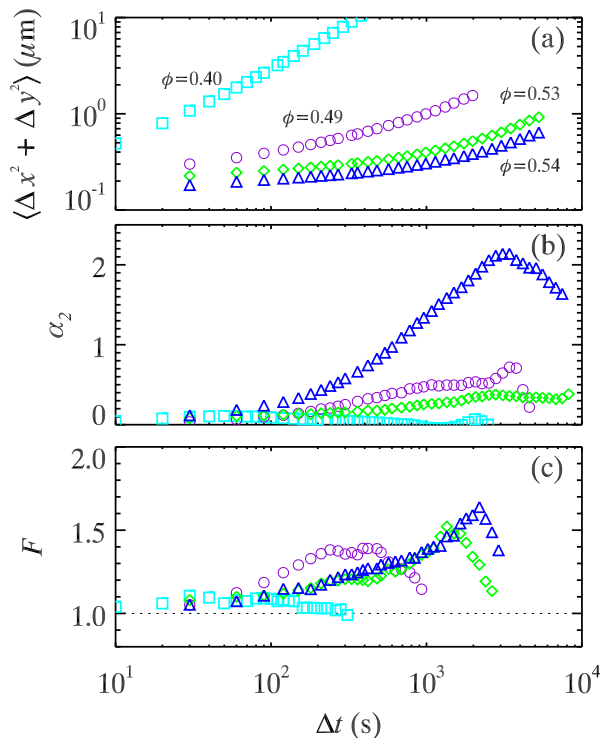


FIG. 2. (color online) (a) Mean-squared displacements (MSD), (b) non-Gaussian parameter and (c) dynamic facilitation parameter of small particles in a bidisperse colloidal suspension with volume fractions indicated in (a). The symbols are the same in all three panels.

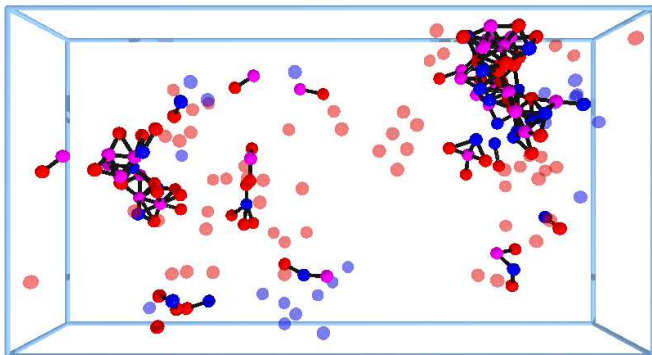


FIG. 3. (Color) Highly mobile (see text) colloidal particles for two successive time intervals. Blue particles are those mobile in the first interval but not the second; red are those not mobile in the first interval but mobile in the second; and violet are those mobile during both intervals. Black bonds connect all particles mobile in the second interval to all neighboring particles mobile during the first interval. Particles not involved in facilitation (as measured by Eqn. 2) are not connected to other particles and drawn slightly transparent. The particles are in their positions at the end of the first interval/beginning of the second interval. Particles not mobile during either interval are not shown. Particles are drawn at 60% of their size. The data correspond to a monodisperse sample with  $\phi = 0.52$ ,  $\Delta t = 600$  s. The displayed volume is  $63 \times 34 \times 11 \mu\text{m}^3$ .

interval between  $t - \Delta t$  and  $t$  and the “future” interval between  $t$  and  $t + \Delta t$  and use Eqn. 1 to compute all particles’ mobilities in these two intervals. We then define “high mobility” particles as those with  $\delta r(\Delta t)$  above a cutoff  $\delta r^*$  such that, over time, 5% of the particles have displacements larger than  $\delta r^*$ ; although at any given moment, the fraction of mobile particles may be more or less than 5% [8, 14, 22]. We are interested in particles with both a low past mobility and a high future mobility, and compute the probability  $p_{LH}$  that these particles have at least one previously high mobility neighbor. The crux of the dynamic facilitation model is that the transition in these particles from low-to-high mobility is brought about by a previous high mobility neighbor. (Nearest neighbors are defined as all particles whose center-of-mass falls within the first minimum  $r_{min}$  of the radial distribution function  $g(r)$ , shown by the solid line in Fig. 4 for a representative sample.)

As in Vogel and Glotzer, we also compute the probability  $p_{LA}$  that a particle with a low past mobility and *any* mobility in the future has a neighbor with previously high mobility and define the facilitation parameter as [14]

$$F(\Delta t) \equiv p_{LH}/p_{LA}. \quad (2)$$

$F$  is a function of the time interval  $\Delta t$  used to define mobility, and the probabilities are computed from all particles and all times  $t$ . If dynamic facilitation is not the mechanism for correlated motion, then particles which become mobile (a low-to-high mobility transition) bear no spatial relation to the previous high mobility particles and  $F(\Delta t) = 1$  ( $p_{LH} = p_{LA}$ ). Instead, as we now describe, we find  $F(\Delta t) > 1$  ( $p_{LH} > p_{LA}$ ), and conclude that dynamic facilitation *is* enabling large-scale particle motions. Conceptually,  $F > 1$  means that the particles connected by black bonds in Fig. 3 are more prevalent than expected by chance.

The resulting facilitation parameter as a function of delay time  $\Delta t$  is shown in Figs. 1(c) and 2(c). For both monodisperse and bidisperse samples the function shows a peak that grows as the glass transition is approached. The time scale  $\Delta t$  of this peak corresponds to that of the peak in the non-Gaussian parameter. Figures 1(c) and 2(c) indicate that, compared to immobile particles, newly mobile particles are almost twice as likely to have a previously mobile particle, quantitatively (as well as qualitatively) similar to the simulations results of Vogel & Glotzer [14]. Thus we find previously mobile particles indeed facilitate the mobility of their neighbors as predicted by Garrahan and Chandler [10, 11]. As a control case, the bidisperse sample with  $\phi = 0.40$  (far from the glass transition) in Fig. 1(c) shows almost no facilitation.

To determine the spatial range over which facilitation occurs we vary the distance  $r$  used to define nearest neighbors. The circles in Fig. 4 show the peak value of facilitation  $F$  as a function  $r$  (using  $\Delta t$  close to the cage-rearrangement timescale  $\Delta t^*$ ). Recall that the peak value

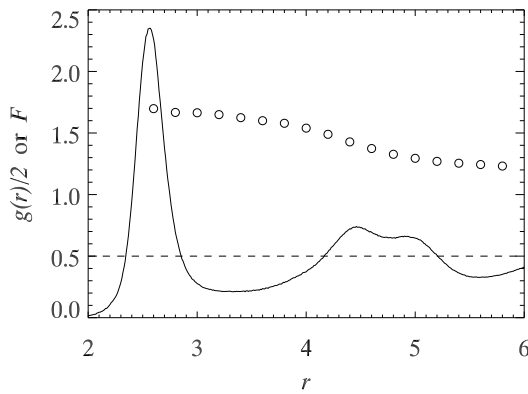


FIG. 4. *Solid line*: Radial distribution function  $g(r)$  (divided by 2 to fit within axes) for a monodisperse sample ( $\phi = 52\%$ ). The function peaks at the particle diameter  $2.36 \mu\text{m}$ . Nearest neighbors are defined as typically defined as all particles whose center-of-mass falls within the first minimum ( $3.4 \mu\text{m}$ ). *Circles*: Peak of dynamic facilitation parameter as a function of  $r$ , defining nearest neighbors as all particles within a distance  $r$ . For these data, the time scale is set to  $\Delta t = 600$  s, which maximizes  $F$  [see diamond symbols in Fig. 1(c)].

of  $F$  indicates the increased probability that a newly mobile particle has at least one previously mobile particle within the distance  $r$ . The largest values of  $F$  are found for  $r \leq 3.4 \mu\text{m}$ , which matches the conventional definition of a nearest neighbor. Figure 4 shows that this enhanced probability decreases with  $r$ , but is still larger than 1 even over distances corresponding to second-nearest neighbors (particles within the 2nd minimum of  $g(r)$ ). The decrease for  $r > 3.2 \mu\text{m}$  shows that, in these colloidal samples, facilitation is primarily through the influence of the nearest neighbor particles.

In summary, we see spatiotemporal correlations of mobility in colloidal samples approaching the glass transition that are the defining feature of dynamic facilitation. Quantitative evidence is seen in a peak in the Vogel-Glotzer parameter close to the rearrangement timescale  $\Delta t^*$ , the time scale for which particle motion is spatially heterogeneous and cooperative [7, 8, 21, 22], and agrees with earlier simulation results. Our new analysis reveals that the spatially correlated motion at a particular time facilitates subsequent motion in adjacent particles, as predicted by the dynamic facilitation model. Our data demonstrate that in samples close to the glass transition, regions of mobility influence subsequent dynamics nearby, rather than mobility arising randomly in new locations. It is precisely these facilitated spatially heterogeneous motions that eventually propagate throughout the sample and allow it to flow, albeit on long time scales for highly viscous samples near the glass transition.

This work was supported by the National Science

Foundation through grants DMR-1133722 (SVF) and CMMI-1250235 (ERW).

\* svfsps@rit.edu

† erweeks@emory.edu

- [1] A. Cavagna, Phys. Rep. **476**, 51 (2009), arXiv:0903.4264.
- [2] M. D. Ediger and P. Harrowell, J. Chem. Phys. **137**, 080901 (2012).
- [3] G. Biroli and J. P. Garrahan, J. Chem. Phys. **138**, 12A301 (2013).
- [4] E. Hempel, G. Hempel, A. Hensel, C. Schick, and E. Donth, J. Phys. Chem. B **104**, 2460 (2000).
- [5] H. Sillescu, J. Non-Cryst. Solids **243**, 81 (1999).
- [6] M. D. Ediger, Ann. Rev. Phys. Chem. **51**, 99 (2000).
- [7] W. Kob, C. Donati, S. J. Plimpton, P. H. Poole, and S. C. Glotzer, Phys. Rev. Lett. **79**, 2827 (1997).
- [8] C. Donati, J. F. Douglas, W. Kob, S. J. Plimpton, P. H. Poole, and S. C. Glotzer, Phys. Rev. Lett. **80**, 2338 (1998).
- [9] M. M. Hurley and P. Harrowell, Phys. Rev. E **52**, 1694 (1995).
- [10] J. P. Garrahan and D. Chandler, Phys. Rev. Lett. **89**, 035704 (2002).
- [11] J. P. Garrahan and D. Chandler, Proc. Nat. Acad. Sci. **100**, 9710 (2003).
- [12] D. Chandler and J. P. Garrahan, Ann. Rev. Phys. Chem. **61**, 191 (2010).
- [13] K. Vollmayr-Lee and E. A. Baker, Europhys. Lett. **76**, 1130 (2006).
- [14] M. Vogel and S. C. Glotzer, Phys. Rev. Lett. **92**, 255901 (2004).
- [15] P. N. Pusey and W. van Megen, Nature **320**, 340 (1986).
- [16] G. L. Hunter and E. R. Weeks, Rep. Prog. Phys. **75**, 066501 (2012).
- [17] Z. Cheng, J. Zhu, P. M. Chaikin, S.-E. Phan, and W. B. Russel, Phys. Rev. E **65**, 041405 (2002).
- [18] W. van Megen and S. M. Underwood, Phys. Rev. E **49**, 4206 (1994).
- [19] G. Brambilla, D. E. M. El Masri, M. Pierno, L. Berthier, L. Cipelletti, G. Petekidis, and A. B. Schofield, Phys. Rev. Lett. **102**, 085703 (2009).
- [20] A. van Blaaderen and P. Wiltzius, Science **270**, 1177 (1995).
- [21] W. K. Kegel and A. van Blaaderen, Science **287**, 290 (2000).
- [22] E. R. Weeks, J. C. Crocker, A. C. Levitt, A. Schofield, and D. A. Weitz, Science **287**, 627 (2000).
- [23] T. Narumi, S. V. Franklin, K. W. Desmond, M. Tokuyama, and E. R. Weeks, Soft Matter **7**, 1472 (2011).
- [24] W. C. K. Poon, E. R. Weeks, and C. P. Royall, Soft Matter **8**, 21 (2012).
- [25] J. C. Crocker and D. G. Grier, J. Colloid Interface Sci. **179**, 298 (1996).
- [26] A. D. Dinsmore, E. R. Weeks, V. Prasad, A. C. Levitt, and D. A. Weitz, App. Optics **40**, 4152 (2001).
- [27] A. Rahman, Phys. Rev. **136**, A405 (1964).